

# Morphology-Dependent Antioxidant Activity of Gold Nanoparticles Prepared Using Different Electrolyte Concentrations

Babay Asih Suliasih and Azri Farhanah\*

Centre for Drug Delivery Technology and Vaccine, Faculty of Pharmacy, Universiti Kebangsaan Malaysia, Kuala Lumpur 50300, Malaysia

\*Corresponding author: p129542@siswa.ukm.edu.my

## Received

21 January 2025

## Received in revised form

19 February 2025

## Accepted

22 February 2025

## Published online

28 February 2025

## DOI

<https://doi.org/10.56425/cma.v4i1.93>



Original content from this work may be used under the terms of the [Creative Commons Attribution 4.0 International License](https://creativecommons.org/licenses/by/4.0/).

## Abstract

Antioxidants play a crucial role in protecting the body from oxidative stress by neutralizing free radicals. The synthesis of antioxidant-active materials, such as gold nanoparticles (AuNPs), offers significant advantages due to their unique physicochemical properties. In this study, AuNPs were successfully synthesized using the electrodeposition method on indium-tin oxide substrates, with varying  $\text{Na}_2\text{SO}_4$  electrolyte concentrations. Scanning electron microscopy analysis confirmed that the synthesized AuNPs exhibited a round to slightly irregular morphology, with an average particle size ranging from 48 to 65 nm. X-ray diffractometer characterization revealed that the nanoparticles possessed a face-centered cubic crystal structure, confirming their high purity. Antioxidant activity was evaluated using the DPPH assay, where AuNPs synthesized with 0.5 M  $\text{Na}_2\text{SO}_4$  exhibited the highest DPPH inhibition of 72.39%. This enhanced antioxidant performance is attributed to the smaller particle size, which increases the available surface area for free radical neutralization. These findings highlight the potential of electrodeposited AuNPs as effective antioxidants and provide valuable insights into optimizing nanoparticle synthesis for biomedical and nanotechnological applications.

**Keywords:** gold nanoparticles, antioxidant activity, morphology, DPPH assays

## 1. Introduction

Free radicals are highly unstable atoms or molecules that pose potential harm to the human body due to their unpaired electrons, which make them highly reactive [1]. This reactivity enables free radicals to interact with biological molecules, potentially leading to cellular damage or the formation of abnormal compounds [2,3]. By attacking surrounding cells, free radicals can initiate further harm, contributing to oxidative stress and various health issues [4,5]. Consequently, extensive research has been conducted to explore the use of antioxidants as a means to counteract the detrimental effects of free radicals [6].

Recent advancements in antioxidant research have been closely linked to developments in nanotechnology, which enhances the active surface area of antioxidant compounds. A larger active surface area significantly increases the reactivity and effectiveness of synthesized

materials [7]. Various metal oxides and metal nanoparticles (NPs) have been widely investigated for their antioxidant potential. Notable studies on ZnO nanoparticles [8,9] have demonstrated promising antioxidant activity. Additionally, other metals such as Pt [10,11],  $\text{Cu}_2\text{O}$  [12–14], Ni [15], and Co [15] have been explored for similar applications. Among these, Au nanoparticles (AuNPs) have emerged as one of the most widely studied due to their remarkable antioxidant properties [16–20].

The use of gold nanoparticles as antioxidants is primarily attributed to their low cytotoxicity, ability to inhibit reactive oxygen species, and proven efficacy in neutralizing free radicals. A study by Patra et al. [21] demonstrated the antioxidant potential of gold nanoparticles synthesized by reducing  $\text{AuCl}_3$  with onion skin extract, achieving an inhibition rate of 14.44% at a concentration of 100  $\mu\text{g}/\text{mL}$ . Additionally, gold nanoparticles synthesized using *C. cuspidatus* extract have

been shown to enhance the antioxidant activity of natural compounds. This is evident in the percentage inhibition values, where the natural extract alone exhibited 96.63% inhibition, which increased to 97.05% when adsorbed onto the surface of AuNPs. This enhancement is attributed to the synergistic effect of the hydrogen donor mechanism of natural compounds and the electron-donating properties of gold nanoparticles [22]. The electron donation process occurs at the nanoparticle surface, where interactions between the unpaired electrons of free radicals and the conduction band electrons of AuNPs facilitate their neutralization [23].

Over the years, various methods for synthesizing gold nanoparticles have been developed. Typically,  $\text{Au}^{3+}$  ions are reduced to zero-valent  $\text{Au}^0$  through chemical reactions with reducing agents such as citric acid, borohydride, or biological reductants derived from natural extracts, fungi, and bacteria [24–26]. However, these chemical methods can negatively impact nanoparticle purity, involve toxic and costly reagents, and pose environmental hazards [27]. An alternative and promising approach for synthesizing gold nanoparticles (AuNPs) is electrodeposition. This method offers several advantages, including a straightforward synthesis process, high purity, precise control over nanoparticle morphology, and the absence of toxic chemicals [28]. Moreover, electrodeposition enables the formation of gold nanoparticles in a solid phase, allowing for the independent evaluation of their antioxidant activity without interference from solution-based reducing agents [29,30].

One of the most effective electrodeposition techniques for gold nanoparticle synthesis is cyclic voltammetry (CV). This method is advantageous as it produces highly pure nanoparticles and allows for precise determination of optimal deposition conditions [31]. Key parameters influencing the quality of AuNPs synthesized via CV include the applied potential range, number of cycles, solution concentration, scan rate, electrolyte composition, pH, and the presence of additives [31,32]. By fine-tuning these parameters, high-quality gold nanoparticles with enhanced antioxidant properties can be successfully synthesized.

## 2. Materials and Method

### 2.1 Materials

All solutions used for electrochemical activity and deposition were prepared using deionized water. The DPPH solution was prepared in ethanol (98% purity, Sigma-Aldrich). The gold precursor,  $\text{HAuCl}_4 \cdot 3\text{H}_2\text{O}$  (99.9% purity, Merck), and the supporting electrolyte,  $\text{Na}_2\text{SO}_4$  (99.0%

purity, Merck), were used for the electrodeposition process.

### 2.2 Methods

#### 2.2.1 Synthesis of AuNPs

Gold nanoparticles (AuNPs) were synthesized via electrodeposition using a potentiostatic technique. A 0.5 mM  $\text{HAuCl}_4$  solution was prepared by dissolving  $\text{HAuCl}_4 \cdot 3\text{H}_2\text{O}$  in deionized water and diluting it with  $\text{Na}_2\text{SO}_4$  as the supporting electrolyte. The electrodeposition was performed in a three-electrode system, where an indium tin oxide (ITO) substrate functioned as the working electrode, platinum (Pt) as the counter electrode, and Ag/AgCl as the reference electrode. The synthesis was carried out at room temperature (25°C) under controlled parameters, as listed in Table 1.

**Table 1.**  $\text{Na}_2\text{SO}_4$  concentrations and CV parameters used in the AuNPs preparation.

Sample code	$[\text{Na}_2\text{SO}_4]$ (M)	Scan rate (mV/s)	$[\text{HAuCl}_4]$ (M)
AuNPs1	0.1	125	0.5
AuNPs2	0.5	125	0.5
AuNPs3	1.0	125	0.5
AuNPs4	1.5	125	0.5

#### 2.2.2 Characterizations

The morphology of the synthesized gold nanoparticles was analyzed using Scanning Electron Microscopy (SEM, Thermo Scientific Quanta 650). Additionally, X-ray Diffraction (XRD, SMARTLAB Rigaku X-ray diffractometer with  $\text{Cu K}\alpha_1$  radiation ( $\lambda = 1.540598 \text{ \AA}$ ), was used to determine the crystallinity and crystal structure of the gold nanoparticles.

#### 2.2.3 Antioxidant activity test

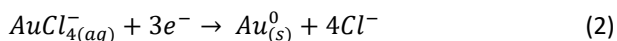
The antioxidant activity of gold nanoparticles was assessed using the 2,2-diphenyl-1-picrylhydrazyl (DPPH) assay. A DPPH solution with a concentration of 39 ppm was prepared, and changes in absorbance were measured using a microplate reader at a wavelength of 516 nm [33]. The antioxidant activity was determined using the following equation (1):

$$\% \text{Inhibition} = \frac{A_0 - A_1}{A_0} \times 100\% \quad (1)$$

where  $A_0$  represents the control absorbance (DPPH solution without nanoparticles), and  $A_1$  is the absorbance after the addition of gold nanoparticles. The inhibition percentage was calculated after 15 minutes to assess the effectiveness of gold nanoparticles as antioxidants.

### 3. Results and Discussion

AuNPs were synthesized by reducing  $\text{AuCl}_4^-$  using the electrodeposition method. The reduced gold atoms were deposited on the ITO-PET substrate. The reduction of  $\text{AuCl}_4^-$  during this process occurs according to the following reaction [34]:



The X-ray diffraction (XRD) pattern of gold nanoparticles synthesized in  $\text{Na}_2\text{SO}_4$  is presented in Fig. 1, confirming their face-centered cubic (FCC) crystal structure. The presence of distinct diffraction peaks indicates the crystalline nature of the synthesized nanoparticles. In a crystalline structure, atoms, ions, or molecules are arranged in a highly ordered, repeating pattern in three dimensions [37]. Reflections were observed at  $2\theta$  values of  $38.27^\circ$ ,  $44.48^\circ$ ,  $64.73^\circ$ , and  $77.76^\circ$ , corresponding to the (111), (200), (220), and (311) lattice planes, respectively. These diffraction peaks align with the reference data from the crystallography open database (COD) No. 96-110-0139 and are consistent with findings reported by Singh et al. [38]. However, a shift in the diffraction peaks was observed when comparing the synthesized nanoparticles to the COD reference. This peak shift can be attributed to variations in lattice structure within the nanoparticle clusters. Differences in lattice spacing influence crystallite size, leading to discrepancies between the synthesized nanoparticles and the reference data. Such shifts in diffraction patterns are common in nanomaterials and can result from strain, lattice distortions, or defects within the crystal structure [36]. These structural differences highlight the impact of synthesis conditions on the crystallinity and size of gold nanoparticles.

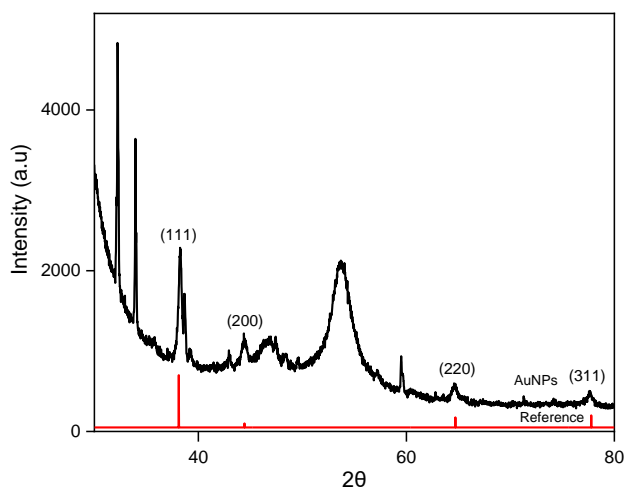


**Figure 1.** X-Ray diffraction pattern of AuNPs.

The morphological characteristics of AuNPs synthesized at varying electrolyte concentrations were analyzed using SEM. Figure 2 presents the morphology of gold nanoparticles prepared with different concentrations of  $\text{Na}_2\text{SO}_4$ , along with a histogram illustrating their size distribution.  $\text{Na}_2\text{SO}_4$  is used to enhance the electrochemical activity of gold, thereby improving the synthesis of the gold film. The SEM analysis of AuNPs synthesized with a  $\text{Na}_2\text{SO}_4$  concentration of 0.1 M (Fig. 2a) reveals that the particles are predominantly round. However, the nanoparticles are sparsely and unevenly distributed, failing to form a dense coverage on the substrate. The corresponding size distribution (Fig. 2e) indicates the presence of relatively few particles, with an average diameter of 48.29 nm. When the  $\text{Na}_2\text{SO}_4$  concentration was increased to 0.5 M, the nanoparticles exhibited a more uniform distribution, with a round to slightly irregular shape. The particle density increased compared to the lower concentration, resulting in an average size of 54.06 nm (Fig. 2b). At a concentration of 1 M  $\text{Na}_2\text{SO}_4$ , the AuNPs formed a highly dense distribution while maintaining a predominantly round morphology, with an average particle size of 65.09 nm (Fig. 2c). This increased density led to significant particle aggregation, contributing to the formation of larger nanoparticles.

**Table 2.** Comparison of  $2\theta$  in this study with COD No.96-110-0139.

COD No.96-110-0139	This study
38,19	38,27
44,39	44,48
64,58	64,73
77,58	77,76

Further increasing the  $\text{Na}_2\text{SO}_4$  concentration to 1.5 M produced larger particles with irregular shapes, Fig. 2d. This irregularity can be attributed to excessive particle density, which promotes aggregation. Aggregation occurs due to the high surface energy of smaller particles; when in close proximity, they tend to coalesce to minimize surface energy, ultimately forming bulk structures [39]. The addition of an electrolyte plays a crucial role in the electrodeposition process of AuNPs by enhancing solution conductivity, facilitating the desolvation of  $\text{AuCl}_4^-$  ions, and improving electron transfer during the reduction process [40]. The  $\text{SO}_4^{2-}$  ion, classified as a kosmotropic ion, stabilizes the electrolyte solution by forming strong interactions with water molecules [41]. As the  $\text{Na}_2\text{SO}_4$  concentration increases, it enhances the distribution of water and metal ions, as well as the interactions between the electrodes. This, in turn, influences the efficiency and

characteristics of nanoparticle deposition at the three-phase interface [42]. Consequently, the nucleation and growth of AuNPs occur more rapidly, leading to the formation of larger particles [43].

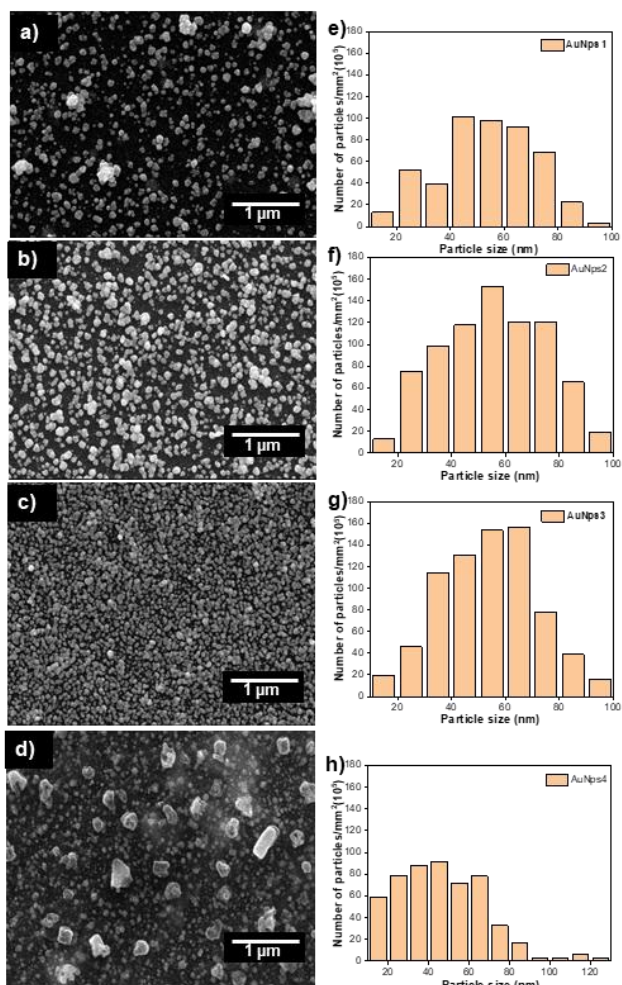


**Figure 2.** SEM micrograph and particle distribution of (a,e) AuNPs1, (b,f) AuNPs2, (c,g) AuNPs3, (d,h) AuNPs4.

The antioxidant activity of the synthesized AuNPs was evaluated using the DPPH assay, with the results presented in Figure 3. Based on the micrographs, AuNPs synthesized in a 0.5 M  $\text{Na}_2\text{SO}_4$  electrolyte solution exhibited the highest inhibition percentage. Additionally, the inhibition percentage increased progressively every 15 minutes. This increase occurs because prolonged exposure allows more gold nanoparticles to interact with free radicals.

Gold nanoparticles synthesized with different  $\text{Na}_2\text{SO}_4$  concentrations were tested to assess how electrolyte concentration influences their antioxidant properties. Figure 3 presents a comparison curve illustrating the relationship between inhibition percentage and  $\text{Na}_2\text{SO}_4$  concentration. The results indicate that the optimal inhibition percentage was achieved at a  $\text{Na}_2\text{SO}_4$

concentration of 0.5 M. Furthermore, the inhibition percentage increased with longer reaction times. This effect is attributed to the extended interaction between nanoparticles and free radicals, allowing for more effective scavenging activity. Additionally, prolonged contact time helps prevent the generation of new free radicals. Certain antioxidants, after neutralizing free radicals, contribute to system stabilization and inhibit further radical formation, thereby prolonging their inhibitory effect [44].

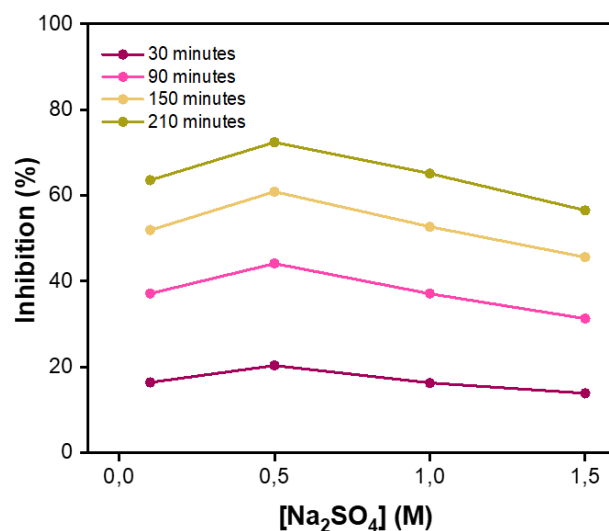


**Figure 3.** Curve depicting the relationship between  $\text{Na}_2\text{SO}_4$  concentration and percent inhibition.

As shown in Table 3, when the  $\text{Na}_2\text{SO}_4$  concentration exceeded 0.5 M, the inhibition percentage declined. Similar to the catalytic activity of AuNPs, antioxidant activity occurs on the nanoparticle surface and is significantly influenced by particle size. Smaller nanoparticles exhibit higher catalytic efficiency due to their larger surface area [45], providing more active sites for interactions with free radicals, thereby enhancing antioxidant performance [43]. This observation aligns with the SEM analysis, which showed that increasing  $\text{Na}_2\text{SO}_4$  concentration led to larger nanoparticle sizes, reducing the overall surface area available for antioxidant interactions and subsequently lowering the inhibition efficiency.

**Table 3.** Percentage inhibition of AuNPs samples in 210 minutes.

Sample	Inhibition (%)
AuNPs1	63.56
AuNPs2	72.39
AuNPs3	65.11
AuNPs4	56.50

#### 4. Conclusion

AuNPs were successfully synthesized using the electrodeposition method with varying  $\text{Na}_2\text{SO}_4$  electrolyte concentrations. The synthesized AuNPs exhibited a predominantly round morphology with slight irregularities and an average particle size ranging from 48 to 69 nm. Antioxidant activity tests using the DPPH assay revealed that AuNPs synthesized with 0.5 M  $\text{Na}_2\text{SO}_4$  (AuNPs3) exhibited the highest DPPH inhibition of 72.39% over 210 minutes. This enhanced antioxidant activity is attributed to smaller particle sizes, which provide a larger surface area for free radical neutralization. These findings highlight the significance of electrolyte concentration in controlling the size, morphology, and antioxidant properties of gold nanoparticles.

#### Author contributions

Babay Asih Suliasih: Writing – original draft, investigation, formal analysis. Azri Farhanah: writing – review & editing, formal analysis.

#### Conflicts of interest

There are no conflicts to declare.

#### Acknowledgement

The authors thank the Center for Science Innovation for providing access to the electrochemical workstation, which facilitated this research.

#### References

- [1] V. Lobo, A. Patil, A. Phatak, N. Chandra, Free radicals, antioxidants and functional foods: Impact on human health, *Pharmacogn. Rev.* **4** (2010) 118–126. <https://doi.org/10.4103/0973-7847.70902>.
- [2] P. Mandal, S.P.S. Babu, N.C. Mandal, Antimicrobial activity of saponins from *Acacia auriculiformis*, *Fitoterapia.* **76** (2005) 462–465. <https://doi.org/10.1016/j.fitote.2005.03.004>.
- [3] A. V Badarinath, K.M. Rao, C. Madhu, S. Chetty, S. Ramkanth, T.V.S. Rajan, K. Gnanaprakash, A Review On In-Vitro Antioxidant Methods: Comparisons, Correlations and Considerations, *Int. J. PharmTech Res.* **2** (2010) 1276–1285. <https://www.sid.ir/en/journal/ViewPaper.aspx?ID=383951>.
- [4] D. Tristantini, A. Ismawati, B.T. Pradana, J. Gabriel, Pengujian Aktivitas Antioksidan Menggunakan Metode DPPH pada Daun Tanjung ( *Mimusops elengi* L ), *Univ. Indones.* (2016) 2.
- [5] O.M. El-Borady, M. Fawzy, M. Hosny, Antioxidant, anticancer and enhanced photocatalytic potentials of gold nanoparticles biosynthesized by common reed leaf extract, *Appl. Nanosci.* **13** (2023) 3149–3160. <https://doi.org/10.1007/s13204-021-01776-w>.
- [6] E.O. Mikhailova, Gold nanoparticles: Biosynthesis and potential of biomedical application, *J. Funct. Biomater.* **12** (2021). <https://doi.org/10.3390/jfb12040070>.
- [7] S. Malinowska, M. Gniadek, T. Rapecki, E. Kurek, Z. Stojek, M. Donten, Polypyrrole–gold nanostructured composite, active and durable electrocatalytic material, *J. Solid State Electrochem.* **18** (2014) 3049–3055. <https://doi.org/10.1007/s10008-014-2408-0>.
- [8] J. Vera, W. Herrera, E. Hermosilla, M. Díaz, J. Parada, A.B. Seabra, G. Tortella, H. Pesenti, G. Ciudad, O. Rubilar, Antioxidant Activity as an Indicator of the Efficiency of Plant Extract-Mediated Synthesis of Zinc Oxide Nanoparticles, *Antioxidants.* **12** (2023). <https://doi.org/10.3390/antiox12040784>.
- [9] N.F.N.S. Fitri, Alsifa Andita Putri, Rachmaniah Nurul Imani, Suci Putriyaningsih, Devia Alventiana Sipayung, Anis Sakinah, Enhancing Antioxidant Activity of Curcumin Using ZnO Nanoparticles Synthesized by Electrodeposition Method, *Chem. Mater.* **2** (2023) 77–81. <https://doi.org/10.56425/cma.v2i3.68>.
- [10] R. Caligiuri, G. Di Maio, N. Godbert, F. Scarpelli, A. Candrea, I. Rimoldi, G. Facchetti, M.G. Lupo, E. Sicilia, G. Mazzone, F. Ponte, I. Romeo, M. La Deda, A. Crispini, R. De Rose, I. Aiello, Curcumin-based ionic Pt(II) complexes: antioxidant and antimicrobial activity, *Dalt. Trans.* **51** (2022) 16545–16556. <https://doi.org/10.1039/d2dt01653b>.
- [11] S. Intarakamhang, A. Schulte, Automated electrochemical free radical scavenger screening in dietary samples, *Anal. Chem.* **84** (2012) 6767–6774. <https://doi.org/10.1021/ac301292c>.
- [12] P.C. Okoye, S.O. Azi, T.F. Qahtan, T.O. Owolabi, T.A. Saleh, Synthesis, properties, and applications of doped and undoped CuO and Cu<sub>2</sub>O nanomaterials, *Mater. Today Chem.* **30** (2023). <https://doi.org/10.1016/j.mtchem.2023.101513>.
- [13] B. Djamila, L.S. Eddine, B. Abderrhmane, A. Nassiba, A. Barhoum, In vitro antioxidant activities of copper mixed oxide (CuO/Cu<sub>2</sub>O) nanoparticles produced from the leaves of *Phoenix dactylifera* L, *Biomass Convers. Biorefinery.* **14** (2024) 6567–6580. <https://doi.org/10.1007/s13399-022-02743-3>.
- [14] M.A. Raihan, S.H. Alfiani, S.P. Chaerani, R.N. Imani,

- Synthesis of Copper ( I ) Oxide Thin Film Through Potentiostatic Electrodeposition as an Antioxidant Film, **3** (2024) 99–107.  
<https://doi.org/10.56425/cma.v3i3.83>
- [15] P. Gull, B.A. Babgi, A.A. Hashmi, Synthesis of Ni(II), Cu(II) and Co(II) complexes with new macrocyclic Schiff-base ligand containing dihydrazide moiety: Spectroscopic, structural, antimicrobial and antioxidant properties, *Microb. Pathog.* **110** (2017) 444–449.  
<https://doi.org/10.1016/j.micpath.2017.07.030>.
- [16] M.H. Moosavy, M. de la Guardia, A. Mokhtarzadeh, S.A. Khatibi, N. Hosseinzadeh, N. Hajipour, Green synthesis, characterization, and biological evaluation of gold and silver nanoparticles using *Mentha spicata* essential oil, *Sci. Rep.* **13** (2023) 1–15.  
<https://doi.org/10.1038/s41598-023-33632-y>.
- [17] Y. Dong, Z. Wang, J. Wang, X. Sun, X. Yang, G. Liu, Mussel-inspired electroactive, antibacterial and antioxidative composite membranes with incorporation of gold nanoparticles and antibacterial peptides for enhancing skin wound healing, *J. Biol. Eng.* **18** (2024) 1–19.  
<https://doi.org/10.1186/s13036-023-00402-3>.
- [18] B.A. Suliasih, A. Sakinah, Marissa Angelina, The Effect of Electrodeposition Voltage on the Antioxidant Activity of Gold Nanoparticles, *Chem. Mater.* **3** (2024) 27–33.  
<https://doi.org/10.56425/cma.v3i1.72>.
- [19] F.G. Milanezi, L.M. Meireles, M.M. de Christo Scherer, J.P. de Oliveira, A.R. da Silva, M.L. de Araujo, D.C. Endringer, M. Fronza, M.C.C. Guimarães, R. Scherer, Antioxidant, antimicrobial and cytotoxic activities of gold nanoparticles capped with quercetin, *Saudi Pharm. J.* **27** (2019) 968–974.  
<https://doi.org/10.1016/j.jsps.2019.07.005>.
- [20] C. Sharma, S. Ansari, M.S. Ansari, S.P. Satsangee, M.M. Srivastava, Single-step green route synthesis of Au/Ag bimetallic nanoparticles using clove buds extract: Enhancement in antioxidant bio-efficacy and catalytic activity, *Mater. Sci. Eng. C.* **116** (2020).  
<https://doi.org/10.1016/j.msec.2020.111153>.
- [21] J.K. Patra, Y. Kwon, K.H. Baek, Green biosynthesis of gold nanoparticles by onion peel extract: Synthesis, characterization and biological activities, *Adv. Powder Technol.* **27** (2016) 2204–2213.  
<https://doi.org/10.1016/j.apt.2016.08.005>.
- [22] M.I. Ponnaniakamideen, S. Rajeshkumar, M. Vanaja, G. Annadurai, In Vivo Type 2 Diabetes and Wound-Healing Effects of Antioxidant Gold Nanoparticles Synthesized Using the Insulin Plant *Chamaecostus cuspidatus* in Albino Rats, *Can. J. Diabetes.* **43** (2019) 82–89.e6.  
<https://doi.org/10.1016/j.jcjd.2018.05.006>.
- [23] J. Beurton, I. Claret, J. Stein, B. Creusot, C. Marcic, E. Marchioni, A. Boudier, Long-lasting and controlled antioxidant property of immobilized gold nanoparticles for intelligent packaging, *Colloids Surfaces B Biointerfaces.* **176** (2019) 439–448.  
<https://doi.org/10.1016/j.colsurfb.2019.01.030>.
- [24] J. Ftouni, M. Penhoat, A. Addad, E. Payen, C. Rolando, J.S. Girardon, Highly controlled synthesis of nanometric gold particles by citrate reduction using the short mixing, heating and quenching times achievable in a microfluidic device, *Nanoscale.* **4** (2012) 4450–4454.  
<https://doi.org/10.1039/c2nr11666a>.
- [25] K. Kalimuthu, B.S. Cha, S. Kim, K.S. Park, Eco-friendly synthesis and biomedical applications of gold nanoparticles: A review, *Microchem. J.* **152** (2020) 104296.  
<https://doi.org/10.1016/j.microc.2019.104296>.
- [26] J. Markus, R. Mathiyalagan, Y.J. Kim, R. Abbai, P. Singh, S. Ahn, Z.E.J. Perez, J. Hurh, D.C. Yang, Intracellular synthesis of gold nanoparticles with antioxidant activity by probiotic *Lactobacillus kimchicus* DCY51T isolated from Korean kimchi, *Enzyme Microb. Technol.* **95** (2016) 85–93.  
<https://doi.org/10.1016/j.enzmictec.2016.08.018>.
- [27] A. Dzimitrowicz, P. Jamróz, G.C. DiCenzo, I. Sergiel, T. Kozlecki, P. Pohl, Preparation and characterization of gold nanoparticles prepared with aqueous extracts of Lamiaceae plants and the effect of follow-up treatment with atmospheric pressure glow microdischarge, *Arab. J. Chem.* **12** (2019) 4118–4130.  
<https://doi.org/10.1016/j.arabjc.2016.04.004>.
- [28] A. Popov, B. Brasiunas, A. Damaskaite, I. Plikusiene, A. Ramanavicius, A. Ramanaviciene, Electrodeposited gold nanostructures for the enhancement of electrochromic properties of panip-dot film deposited on transparent electrode, *Polymers (Basel).* **12** (2020) 1–14.  
<https://doi.org/10.3390/polym12122778>.
- [29] Y. Mukouyama, Y. Fukuda, T. Nishimura, A Simple Electrochemical Method for Preparing Gold Nanoparticles on Graphite, *ECS Trans.* **80** (2017) 1425–1431.  
<https://doi.org/10.1149/08010.1425ECST/XML>.
- [30] Y. Mukouyama, Y. Fukuda, H. Okada, M. Saito, T. Nishimura, Fabrication of Uniformly Sized Gold

- Nanoparticles on Glassy Carbon by Simple Electrochemical Method, *J. Electrochem. Soc.* **166** (2019) D669–D675. <https://doi.org/10.1149/2.1231913jes>.
- [31] M. Yashini, S. Shanmugasundaram, Optimization of parameters influencing the electro-deposition of Gold nanoparticles on electrode using Taguchi method, ~ 2023 ~ *Pharma Innov. J.* **10** (2021) 2023–2030. <http://www.thepharmajournal.com>.
- [32] N.D. Zakaria, M.H. Omar, N.N. Ahmad Kamal, K. Abdul Razak, T. Sönmez, V. Balakrishnan, H.H. Hamzah, Effect of Supporting Background Electrolytes on the Nanostructure Morphologies and Electrochemical Behaviors of Electrodeposited Gold Nanoparticles on Glassy Carbon Electrode Surfaces, *ACS Omega.* **6** (2021) 24419–24431. <https://doi.org/10.1021/acsomega.1c02670>.
- [33] D.I. Syafei, Antioxidant Activity of AuPt Nanoparticle with Square-Wave Pulse Deposition Method, **3** (2024) 39–44. <https://doi.org/10.56425/cma.v3i2.79>.
- [34] N.D. Zakaria, M.H. Omar, N.N. Ahmad Kamal, K. Abdul Razak, T. Sönmez, V. Balakrishnan, H.H. Hamzah, Effect of Supporting Background Electrolytes on the Nanostructure Morphologies and Electrochemical Behaviors of Electrodeposited Gold Nanoparticles on Glassy Carbon Electrode Surfaces, *ACS Omega.* **6** (2021) 24419–24431. <https://doi.org/10.1021/acsomega.1c02670>.
- [35] A.M. Alkilany, C.J. Murphy, Toxicity and cellular uptake of gold nanoparticles: What we have learned so far?, *J. Nanoparticle Res.* **12** (2010) 2313–2333. <https://doi.org/10.1007/s11051-010-9911-8>.
- [36] A.I.A. Rani, B.K. Ghosh, K.A. Mohamad, F. pien Chee, (Pdf) Current Advances in Microdevices and Nanotechnology, 2019. [https://www.researchgate.net/publication/332963107\\_CURRENT\\_ADVANCES\\_IN\\_MICRODEVICES\\_AND\\_NANOTECHNOLOGY](https://www.researchgate.net/publication/332963107_CURRENT_ADVANCES_IN_MICRODEVICES_AND_NANOTECHNOLOGY).
- [37] B.A. Nogueira, C. Castiglioni, Raman Spectroscopy of Crystalline Materials and Nanostructures, *Crystals.* **14** (2024) 5–7. <https://doi.org/10.3390/cryst14030251>.
- [38] M. Singh, R. Kalaivani, S. Manikandan, N. Sangeetha, A.K. Kumaraguru, Facile green synthesis of variable metallic gold nanoparticle using *Padina gymnospora*, a brown marine macroalga, *Appl. Nanosci.* **3** (2013) 145–151. <https://doi.org/10.1007/s13204-012-0115-7>.
- [39] W. Zhang, Nanoparticle aggregation: Principles and modeling, *Adv. Exp. Med. Biol.* **811** (2014) 20–43. [https://doi.org/10.1007/978-94-017-8739-0\\_2](https://doi.org/10.1007/978-94-017-8739-0_2).
- [40] N.D. Zakaria, M.H. Omar, N.N. Ahmad Kamal, K. Abdul Razak, T. Sönmez, V. Balakrishnan, H.H. Hamzah, Effect of Supporting Background Electrolytes on the Nanostructure Morphologies and Electrochemical Behaviors of Electrodeposited Gold Nanoparticles on Glassy Carbon Electrode Surfaces, *ACS Omega.* **6** (2021) 24419–24431. <https://doi.org/10.1021/ACSOMEGA.1C02670>.
- [41] S. Christau, T. Moeller, J. Genzer, R. Koehler, R. Von Klitzing, Salt-Induced Aggregation of Negatively Charged Gold Nanoparticles Confined in a Polymer Brush Matrix, *Macromolecules.* **50** (2017) 7333–7343. <https://doi.org/10.1021/acs.macromol.7b00866>.
- [42] M.Z. Iqbal, Rafiuddin, Structural, electrical conductivity and dielectric behavior of Na<sub>2</sub>SO<sub>4</sub>-LDT composite solid electrolyte, *J. Adv. Res.* **7** (2016) 135–141. <https://doi.org/10.1016/j.jare.2015.04.002>.
- [43] S.A. Akintelu, B. Yao, A.S. Folorunso, Bioremediation and pharmacological applications of gold nanoparticles synthesized from plant materials, *Heliyon.* **7** (2021) e06591. <https://doi.org/10.1016/j.heliyon.2021.e06591>.
- [44] D. Bešlo, N. Golubić, V. Rastija, D. Agić, M. Karnaš, D. Šubarić, B. Lučić, Antioxidant Activity, Metabolism, and Bioavailability of Polyphenols in the Diet of Animals, *Antioxidants.* **12** (2023) 1–27. <https://doi.org/10.3390/antiox12061141>.
- [45] S.H. Brodersen, U. Grønbjerg, B. Hvolbæk, J. Schiøtz, Understanding the catalytic activity of gold nanoparticles through multi-scale simulations, *J. Catal.* **284** (2011) 34–41. <https://doi.org/10.1016/j.jcat.2011.08.016>.